# Variability in ETAS parameters depending on estimation algorithms

*Yuta Mitsui[1], Jun Kataoka[2]

1.Department of Geosciences, Shizuoka University, 2.Faculty of Science, Shizuoka University

The ETAS model (Ogata, 1988) allows us to estimate background seismicity \mu without aftershock effects from an earthquake sequence. As an interesting example, Llenos et al. (2009) showed that slow tectonic deformation truly increased the background seismicity \mu but did not correlate with the other ETAS parameters about aftershock productivity. Several studies such as Ide et al. (2013) expanded in application Kataoka and Mitsui (2015, JpGU) tested this concept for some regions around Japan, and obtained implications for magma intrusion beneath Mt. Fuji after the 2011 Tohoku Earthquake, slow slip events at subduction zones, and attenuation of slow slips after large earthquakes.

For the above parameter estimation, we used SASeis2006 by Ogata (2006). SASeis2006 adopted the DFP method, a kind of quasi-Newton method. However, Kasahara and Yagi (2015, SSJ) constructed a new estimation algorithm based on Newton method and showed a margin for improvement in SASeis2006 especially in terms of initial value dependence.

On the basis of this situation, this study introduce four estimation methods and examine the variability in the estimation results. Namely, we compare the estimation results from the same initial values: (1) downhill simplex method (2) conjugate gradient method (3) quasi-Newton method (BFGS method) with parameter constraints (all parameters are limited in a range of 0.01~10) (4) Newton method. We use earthquakes around Japan (M>2) in the JMA hypocenter catalogue. The time range is every one year in 1998~2014. The spatial range is around the source region of the 1993 southwest-off Hokkaido earthquake and the 2003 Tokachi-oki earthquake.

We find that the solutions do not converge in some cases, especially of SASeis2006 or the Newton method. Moreover, we obtain the following results: [1] Variability in the estimated value of \mu is relatively smaller. The ratio of the maximum value to the minimum value is at most 1.8 times. [2] Variability in the estimated values other than \mu are far larger. The ratio of the maximum value to the minimum value often reaches 10 times, or greater. [3] When comparing among the log-likelihood functions for the estimated parameters, the Newton method accounts for approximately 65% of the maximum likelihood. The conjugate gradient method and the downhill simplex method follows.

Keywords: Seismicity, ETAS model, Parameter estimation

 

# Mutation('08/10,'14/10) of aftershock activity of the 2004 off Kii Peninsula E.q., and Stress structure around the Trough

*Hirofumi Mase[1]

1.none

(Please refer to the Fig.) Because mantle that heads eastward under Chugoku-district pushes the edge of the subducting slab under Kinki-district, the slab tries to creep up and turn to the right by lateral-fault type(1). Two seamounts in the near south of Nankai Trough concentrate this stress like stake. After the north side of the seamounts was destroyed by the earthquake in 2004, the route that power is transmitted to them changed from "from North" to "from Northwest"(2). The aftershocks which still continue at present should change from digestion of the one which was left without breaking by mainshock into something the pressure from the northwest causes. I studied the changes to time passing.
(short circuit in October,2008)A fluctuation occurred at the beginning of October,2008 (Fig.2,3). There were lots of shocks in front of the seamounts in the plane plan. Those seem to have rushed into the south including space between the seamounts. This space would increase in the pressure. I tied first 6 of October to the occurrence order and got a straight line in front of seamount EM. I call the power concentrating at two seamounts at the northwest-southeast direction the northwest compression force NWF(W),NWF(E). (before the main shock,the north compression force NF(W),NF(E))
The state that shocks formed a bend, stood and reached the limit can be judged by the section. NWF(W),NWF(E) produced the new stress-transfer-face which developed to the lower part.
(short circuit in October,2014)The 2nd time of fluctuation is the beginning of October,2014 (Fig.4,5,6). I attached the date of occurrence to something in October and tied something to march with a line (Fig.4). I assigned the number to something important in the occurrence order. The line(encircled number3-1-5-6) which develops in front of seamount EM and the line(encircled number2-4) issued from seamount WM and tries to cross at right angles at the overhead crossing showed. I call compression force about the latter(encircled number2-4) synthetic compression force SWF(W),SWF(E).
I think NF is 0 and the reaction SF decreases at present and NWF is biggest and the reaction SEF is increased at present. The powers work in two seamounts is SWF, resultant of SF,NWF,SEF(Fig.8). The surrounding ground supports a stake after all. Because the seamount gets reaction by its move from the bottom of the sea, the seamount delays to react upon the sudden change of force.
(below,Fig.7)After short circuit in October,2008(the 2nd, 3rd period) it increases in the pressure between the two seamounts, so the pressure rises more and causes destruction effectively at the direction where SWF(W) pushes seamount WM. This is the background where the stress-transfer-face(line,encircled number2-4) appeared, and SWF(W) and NWF(E) intersected with the overhead crossing (the 3rd period).
There is a comment that stress field in the plate in the focal region crosses at right angles mostly in the convergence (the northwest) direction(6). I think this caught the earthquake generating stress that SWF(W) causes.
(1)MASE/JpGU2014/SSS29-P10 (2)MASE/JpGU2015/SSS30-P01 (4)AIST/Visualization system for subsurface structures/all-Japan hypocenter catalog by the JMA/above M1 (5)JHOD,JCG/Seafloor Topography of the Plate Boundaries (6)JAMSTEC/Nakano,Hori/SSJ2014/A22-07/Tectonic background of the 2004 off the Kii Peninsula earthquakes

 

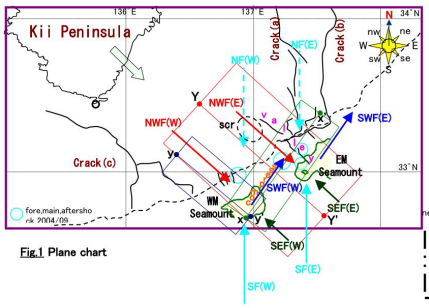


Fig.1 Plane chart

Stress which operates on Seamount

| name | direction | size: until 2004/09 | size: after 2004/09 | cause of appearance |
|---|---|---|---|---|
| NF | from the north | biggest | 0 | edge of slave is repelled |
| SF | from the south | biggest | It decreases | reaction of NF |
| NWF | from the northwest | 0 | biggest | edge of slave is repelled |
| SEF | from the southeast | 0 | It increases | reaction of NWF |
| SWF | It's changing | — | It's changing | resultant of SF,NWF,SEF |

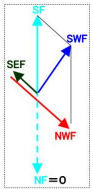


Fig.8

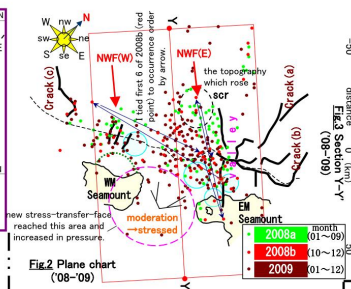


Fig.2 Plane chart ('08-'09)

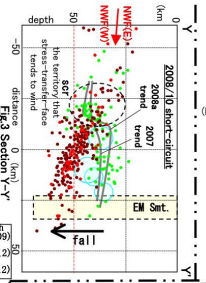


Fig.3 Section Y-Y' ('08-'09)

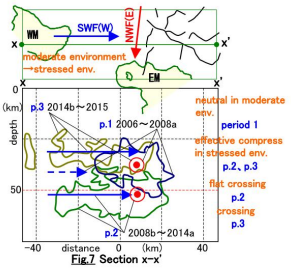


Fig.7 Section x-x'

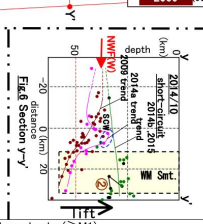


Fig.6 Section y-y'

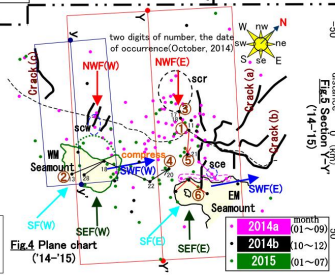


Fig.4 Plane chart ('14-'15)

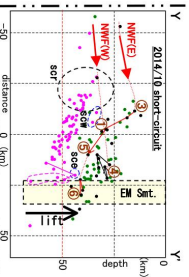


Fig.5 Section Y-Y' ('14-'15)

・small circles : shocks (≧M1) referable to (4)/shifted 10km to the southeast
・about sea bottom (shape line) extracted from (5)

 

# Depth-dependent periodic change in the interplate coupling at NE Japan inferred from spatial gradient of velocity field

*Takeshi Iinuma[1]

1.Japan Agency for Marine-Earth Science and Technology

Surface velocity field of an island arc based on terrestrial GNSS observations includes the effect of the interplate coupling between the overriding continental plate to which the island arc belongs and oceanic plate that is subducting from a trench or a trough. In the Japanese Islands, many studies have been carried out to estimate the distribution of interplate coupling using the surface velocity fields based on the GNSS observations with a dense nationwide observation array [e.g., *Ito et al.*, 1999, 2000; *Mazzoti et al.*, 2000; *Nishimura et al.*, 2004; *Suwa et al.*, 2006; *Hashimoto et al.*, 2009; *Loveless and Meade*, 2010]. However, especially in northeast Japan, it is difficult to resolve the distribution of the interplate coupling along the direction normal to the Japan Trench based on the terrestrial geodetic data, because the trench where the subduction starts is too far (> 200 km) from the land. The spatial change in the degree of coupling is also hard to detect accurately far off the Pacific coast.
*Uchida et al.* [2016] revealed that the interplate coupling between the subducting Pacific and overriding continental plates at the northeast Japan subduction zone periodically changes with the repeat intervals from 1 to 6 years based on the analyses of the small repeating earthquakes and of surface displacement rate field. They applied a geodetic data processing for monitoring the spatio-temporal variation of interplate coupling with calculating the spatial gradient of the surface horizontal velocity field within belt-like zones that are taken along the direction perpendicular to the trench axis. Temporal change in the interplate coupling is detected with shifting the one-year time window in which the surface velocity field is estimated by one week, and spatial variation along the trench-parallel direction is deduced with shifting the latitude of the belt-like zone whose width is 60 km by 0.1 degree. They suggested that the gradient of the horizontal surface velocity depends mainly on the strength of the interplate coupling in shallow portion of the offshore plate interface, while it is still difficult to resolve the distribution of coupling zone on the plate interface and to estimate the temporal change in the degree of coupling in a quantitative manner.
The results of *Uchida et al.* [2016] with respect to the small repeating earthquakes implies that the spatial variation of repeating period of the slow slip on the plate interface depends on the depth, that is, the slow slip occurs with shorter recurrence interval at the deep portion than that at the shallow portion along each profile perpendicular to the trench. In this study, I examined the depth dependency of the repeating period of the slow slip on the plate interface by comparing the predominant periods of the temporal changes in the horizontal and vertical gradients of surface velocity field. *Iinuma et al.* [2010, 114th Meeting of the Geodetic Society of Japan] revealed that the sign of the vertical velocity gradient indicates the presence or absence of interplate coupling at deeper (>50 km) regions of the plate interface beneath the land. It means that the spatial gradient of the vertical velocity field is sensitive to the change in the interplate coupling at the deep portion, while the horizontal component is sensitive to the interplate coupling change at the shallow portion. The result of the examination shows that the predominant period of the temporal change in the vertical velocity gradient is shorter than that in the horizontal component at the most profiles. I will performing comprehensive numerical tests to examine the sensitivities of the spatial gradients of horizontal and vertical velocity fields to the interplate coupling at various depth ranges, and report the quantitative evaluation of the depth dependency of the cycle

 

of the periodic change in the interplate coupling.

Keywords: Interplate coupling, GPS, Northeast Japan, Slow slip event, mega-thrust earthquake, The 2011 off the Pacific coast of Tohoku earthquake

 

# Spatial distribution of stress orientations in Southwestern Japan and its implication for the strength of the median tectonic line

*Keisuke Yoshida[1], Eiichi Fukuyama[1]

1.National research institute for earth science and disaster prevention

In Japan, many devastating earthquakes have historically occurred. There exist many active faults which may cause M>7 inland earthquakes in southwestern Japan. The Median Tectonic line (MTL) is one of the most active inland faults. Because of its large length, MTL has the potential to produce a very large earthquake. It is suggested from GPS analyses that steady aseismic slip at depth (>15 km) has continued to load shear stress on the shallower part of the fault plane of the MTL [Tabei et al., 2002]. In this study, we analyzed focal mechanism data to constrain stress and friction parameters of the MTL.
First of all, we determined focal mechanism solutions by using first-motion polarity data picked by Hi-net. We beforehand selected events with more than 15 first-motion polarity data, and searched acceptable nodal planes for each earthquake which can explain more than 90% of the first-motion data. We then omitted poorly-constrained focal mechanism of which RMS of acceptable nodal planes are more than 30°. As a result, we obtained 25,882 focal mechanisms data for the period between 2001 and 2015. This is 10 times as many as those listed in JMA catalogue. We then selected 14,460 focal mechanisms which occurred shallower than the plate boundary.
Next, we applied the stress tensor inversion method to this data set to investigate the detailed distribution of stress orientations. We first applied the stress tensor inversion developed by Michael [1987] to all the data. The estimated orientation of σ1-axis is WNW-ESE and the stress regime is strike-slip. This orientation largely differs from the orientations of the strain-rate and the relative plate movement as shown in previous studies [e.g. Wang, 2000]. One possible explanation is the effect caused by the collision between northeast and southwest Honshu. This stress orientation is unfavorably-oriented [Sibson, 1985] for the activation of the MTL.
Furthermore, we investigated the spatial distribution of stress orientations by using the following three approaches to subdivide the focal mechanisms catalogue: (a) employed a nonhierarchical clustering algorithm K-means,(b) assigned the focal mechanisms to each meshes with a 1.0° spacing, and (c) assigned the nearest 15-30 focal mechanisms to each grid node with a 0.1° spacing. In all cases,σ1-axes were estimated to be E-W in most of regions. However, the σ1-axes oriented NE-SW in the San-in region as shown in Kawanishi et al. [2009] based on the temporary seismic network data. This regions is situated highly strain concentration zone (Nishimura, 2014), and the orientations of stress is similar to that of the strain rate. Also, σ1-axis is oriented NW-SE in northern Shikoku. In this region, seismic activity is seen along the north-dipping MTL [Sato et al., 2015]. The focal mechanisms have a large diversity there. In Kii-Peninsula, the reverse fault stress regime was estimated. This distribution seems to correspond to the surface topography as seen in northeastern Japan [Yoshida et al., 2015]
The σ1-axes estimated along the MTL are oriented E-W, which are unfavorably-oriented for the reactivation on the MTL. We calculated the upper bound of the apparent frictional coefficient of the MTL to become easier to reactivate rather than form a new optimally oriented fault in intact crust. Estimated upper bound of the apparent frictional coefficient is less than 0.4 along most of the segments, which suggest the MTL is weak.

Keywords: The Median Tectonic line, stress, frictional strength, seismicity

 

 

# Estimate of the stress state in earthquake source region in South African deep gold mine by DCDA

*Shuhei Abe[1], Yasuo Yabe[1], Takatoshi Ito[2], Masao Nakatani[3], Gerhard Hofmann[4], Hiroshi Ogasawara[5]

1.Research Center for Prediction of Earthquakes and Volcanic Eruptions, Graduate School of Science, Tohoku University, 2.Institute of Fluid Science, Tohoku University, 3.Earthquake Research Institute, the University of Tokyo, 4.Senior Mine Seismologist Rock Engineering, 5.Faculty of Science and Engineering, Ritsumeikan University

In the earthquake preparation process, the strength of a fault and the stress state around the fault evolve by interacting with each other through the fault slip. Therefore, many attempts have been done to measure the stresses around faults by deep drillings. However, techniques that are applicable to a large depth (> 1km) are limited. An earthquake of Mw2.2 (mainshock, hereafter) occurred at 3.3km depth in Mponeng mine, a deep gold mine in South Africa. The rupture plane of the mainshock diagonally cut a 30-m-thick gabbroic dike. Yabe et al. (2013) drilled a borehole passing the source fault of mainshock ~1.5 yrs afterward. They constrained possible ranges of the stress magnitudes, as well as the principal directions, based on the criteria of the borehole breakout and the core disking. In this study, we estimate the differential stress in a plane normal to the borehole axis with a higher resolution by Diametrical Core Deformation Analysis (DCDA, Funato and Ito, 2013) to the cores recovered from the borehole. DCDA is applied also to the cores of another borehole drilled ~7 mo before the mainshock in the same area. We also discuss applicability of DCDA to estimate stress at great depths.

DCDA estimates the differential stress from azimuthal variation in diameter (differential strain) of a core induced by stress relief associated with drilling. We collected seven core samples, ~30 cm long, from each borehole. The diameter was measured along circumferential profile lines set every ~2 cm on each core. Results: Coherent azimuthal variations in diameter were seen on three and five of seven core samples collected from the borehole drilled before and after the mainshock, respectively. Since core samples with incoherent diameter variations are considered to be damaged during drilling, we exclude them from the discussion below.

The pre-mainshock differential stresses were estimated to be ~100 MPa along the borehole from the central part of the dike to the host rock (quartzite) in west. The post-mainshock ones were about 20 MPa in the western host rock and near the west contact. On the other hand, it was ~70 MPa at the central part of the dike. The post-mainshock differential stresses obtained in this study fell in the range estimated by Yabe et al. (2013), while they were two times or more greater than their optimal values.

In DCDA, it is assumed that the core expansion induced by the stress relief by drilling is purely elastic. However, the core samples in this study were taken at a depth of ~3.3 km from the surface. The overburden pressure is as high as ~80 MPa. When such a high stress as ~80 MPa is unloaded, the inelastic deformation may occur, resulting in overestimation of the differential stress. In order to evaluate the effect of the inelasticity on the estimation, we carried out uniaxial creep tests of the dike. The ratio of the inelastic deformations to the elastic deformations was less than 10%. Just before the yielding under the uniaxial compression test or the uniaxial tensile (Brazilian) test, the inelastic strains were not larger than 30 % of the elastic strains. Therefore, the larger magnitudes of the differential stresses estimated in this study than those by Yabe et al. (2013) are not apparent by the inelasticity of the dike. There is a significant difference between the pre- and the post-mainshock differential stresses. However, because of different inclinations of the two boreholes, the pre- and the post-mainshock differential stresses cannot directly be

 

compared with each other. We grid-searched a stress state that can reproduce both differential stresses. The principal directions of stress were fixed to those by Yabe et al. (2013). The maximum magnitude of the principal stresses was 300 MPa. No stress state was found to simultaneously reproduce both of the pre- and the post-mainshock differential stresses, suggesting that DCDA can detect a temporal change in the stress state.

Keywords: South African deep gold mine, Diametrical Core Deformation Analysis

 

# Searching largest displacement zone of the 2014 Orkney earthquake fault with strain data and using Map3Di for scientific drilling.

*Akimasa Ishida[1], Hiroshi Ogasawara[1], Hiroyuki Ogasawara[1], Taka Uchiura[1], Raymond Durrheim[2,3], Alex Milev[3], Makoto OKUBO[4], Teruhiro Yamaguchi[5]

1.Ritsumeikan University , 2.Univ. Witwatersrand, South Africa, 3.CSIR, South Africa,, 4.Kouchi University, 5.Hokkaidou University

The largest event recorded in a South African gold mining region, a M5.5 earthquake took place near Orkney on 5 August 2014. This is one of the rare events as the main- and after-shocks were recorded by 46 geophones at 2-3 km depths, 3 Ishii borehole strain meters at 2.9km depth, and 17 surface strong motion meters at close distances. The upper edge of the planar distribution of aftershock activity dipping almost vertically was only some hundred meters below the sites where the strainmeters were installed at distances larger than a few tens of meters from tunnel. A scientific project is planned to drill into the 2014 Orkney earthquake fault from the localities near the strain meter sites. It is a rare opportunity to recover fault material and fractures, to measure stress, to monitor after drilling at the M5.5 seismic zone.The final purpose of our research is to understand how main rupture stopped and why aftershock have occurred in sequence as observed. For this purpose, we attempted to constrain the largest displacement zone of the 2014 Orkney earthquake fault that account for the observed co-seismic strain with Map3Di to suggest where to drill. We checked polarities of each component of the strainmeters by comparing the observed tidal change with theoretically calculated tide Gotic2 [Sato and Honda (1984)], modifying the polarities of a few components with problems. Identical responses were recorded with the three strainmeters to a M4 earthquake at a few km distance, whereas .much larger (up to 1e-5) and different responses were recorded to the M5.5 earthquake.We calculated strain change of each component of the three strain meters by assuming uniform fault slip over a rectangle area with a same aspect ratio of aftershock area with various areas using map3Di. We found the rectangular area with a uniform fault slip of 0.5 m can explain the observed magnitudes of strain changes. However, we haven’t yet evaluated local effects that might cause discrepancies in each component of the three strainmeters. At Japan Geoscience Union Meeting 2016, we are going to make a follow-up report.

Keywords: South Africa, Boundary element method, Drilling project, Strain data, Seismogenic zones

 

# Spatio-temporal variation of the stress drop revealed the generation and migration process of the 2009 swarm activity at Hakone volcano

*Miyu Fujioka[1], Yohei Yukutake[2], Ahyi KIM[1]

1.yokohama city university, 2.Hot Springs Research Institute of Kanagawa Prefecture

Hakone volcano has been an active volcano which is started about 400 thousands years ago. In addition the volcanic activity has caused seismic swarm periodically. Since those swarm activity occasionally generate widely felt earthquake, it is important to elucidate the generation process of the activity for future disaster mitigation. Yukutake et al. (2011) performed precise relocation of 2009 Hakone swarm hypocenters and found that a clear migration of the hypocenters which is consistent with diffusion of pressurized thermal fluid. However, it is still unclear 1) how the fluid controls the initiation of the swarm, and 2) whether all earthquakes during the sequence occurred under the same generation process.
In this study, to address the questions, we estimated the stress drop of the earthquakes observed during the 2009 sequence using empirical Green's function deconvolution method. Obtained stress drop were generally low, ranging between 0.01 MPa to 0.1 MPa, indicating the pore pressure increase might get involved the activity. Furthermore, the result showed the clear spatio-temporal variation of the stress drop: The stress drop tends to be higher when it occurs earlier and closer to the hypocenter of the initial earthquake. It implies that the flow of highly pressurized fluid initiated the swarm and promoted at the initial stage of seismic activity. However, at the middle to last stage, earthquakes might be triggered by pore pressure increase and/or stress perturbation due to the occurrence of the events earlier.

Keywords: Hakone volcano, swarm earthquakes, empirical Green's function method, stress drop, invaginated the fluid

 

# Early rupture process of 14 March 2014 Iyo-Nada intermediate-depth earthquake inferred from 3D and 2D source imagings

*Takamasa Usami[1], Masanao Komatsu[1], Hiroshi Takenaka[1]

1.Graduate School of Natural and Technology, Okayama University

An intermediate-depth earthquake ($M_{JMA}$ 6.2) occurred in Iyo-Nada on March 14, 2014. The focal depth is estimated to be 78 km by JMA, and this event occurred in the Philippine Sea slab. In this study, we investigate the early rupture process of the earthquake for three seconds after the initial break. We use P-wave portion on vertical components of waveform records at 50 seismic stations from the seismic networks of JMA, NIED, and AIST. The result of three-dimensional (3D) imaging, we find three strong slip regions S1, S2, and S3 except the hypocenter (S) corresponding to the initial break: S1 is located close to S, northward and upward from the hypocenter at about 0.7 seconds after the initial break, S2 about 9 km southward and 6 km downward at about 2.2 seconds after the initial break, and S3 about 8 km eastward and 7 km downward at about 2.7 seconds after the initial break. From this result, we suggest a fault model with two planes: initial rupture plane including S and S1 with strike of 22°E and dip angle of 69° from JMA's P-wave first motion focal mechanism and the main rupture plane including S2 snd S3 with strike of 244°E and dip angle of 26° from JMA's CMT solution. Then, from the two-dimensional (2D) imaging, we locate the main rupture plane to be 7 km just below the hypocenter. The rupture process is interpreted as follows: a large slip occurred at S1 close to the hypocenter on the initial plane; after the rupture propagated southward and downward on the initial plane and got into the main rupture plane, another large slip occurred at S2; asides, the third large slip then took place at S3.
Acknowledgments: we used the strong motion records of JMA, NIED, and AIST.

Keywords: Initial rupture, Main rupture, Source imaging, 2014 Iyo-Nada intermediate-depth earthquake

 

# What caused the unusual Non-DC component observed in the Jan. 28th 2012 Tanzawa earthquake?

*Shinji Sato[1], Ahyi KIM[1]

1.Yokohama City University

The Tanzawa mountain area is seismically very active: the seismicity in the western Tanzawa is mainly caused by collision of the Izu peninsula and that of the eastern part is caused by subduction of the Phillipine sea plate. Especially in the western part, magnitude (M) ~ 5 earthquake which accompanies similar sized foreshock has been periodically observed. The cause of foreshock is still controversial. The last seismic activity in this region was on Janualy 2012; the M5.4 mainshock occurred on January 28th followed by its M4.7 foreshock occurred 4 minutes later and the aftershock sequence lasted 13 days. One interesting observation of the sequence was that the both foreshock and mainshock exhibited unusual amount of CLVD component whereas similar sized after shock showed nearly pure double couple. The results of the moment tensor inversion using precisely determined hypocenter location and moment rate function analysis indicated that the complex faulting system in the hypocentral area caused the large CLVD. It is consistent with the mechanism differences between ~ M5 earthquakes observed during the sequence. It implies there is a relationship between the complex faulting system and the triggering mechanism of the foreshock.

Keywords: Tanzawa mountain, mechanism, CLVD component, moment tensor inversion, moment rate function

 

# Characteristics of the rupture processes of two large earthquakes off the south-east Kushiro area in Hokkaido in 2004

*Tomoyuki Sagawa[1], Yuichiro Tanioka[1], Takuji Yamada[2]

1.Institute of Seismology and Volcanology, Department of Natural History Sciences,Graduate School of Science,Hokkaido University, 2.Ibaragi University

In this study, Source processes of two Kushiro-oki earthquakes, which occurred in November and December, 2004 (Mw7.1 and Mw6.9), are analyzed. These earthquakes occurred with short time interval and with short distance separation at the same plate boundary. In 1961, two earthquakes of M7 also occurred with a time difference of 3 months at the same plate boundary. In addition, this plate boundary is surrounded by the source area of the large earthquakes of M8, such as the 1973 Nemuro-oki earthquake and the 2003 Tokachi-oki earthquake. Therefore, it is important to study source characteristics of two 2004 Kushiro-oki earthquakes in order to understand the complexity of the plate interface.

We estimate the source time function at each strong motion station (K-net) using empirical green's function method. Then, the directivity effect is analyzed from those estimated source time functions. In consequence, the result suggests that the rupture propagated concentrically for the earthquake occurred in November and propagated about 8 km to the north for the earthquake occurred in December. Moreover, for the earthquake occurred in December, the stress drop was found to be uniform, because few aftershocks occurred within the source area of the earthquake. The earthquake occurred in November affected by the postseismic slip of the Tokachi-oki earthquake. Because the earthquake occurred in December did not increase enough stress at the edge of the source area of the 1973 Nemuro-oki earthquake, the rupture propagated to the north in stead of to the south.

Keywords: 2004 Kushiro-oki earthquake, source process

 

# Dynamic rupture model of the 2014 northern Nagano, central Japan, earthquake (Part 3)

*Yuko Kase[1]

1.Geological Survey of Japan, AIST

We construct a dynamic rupture model of the 2014 northern Nagano, central Japan, earthquake to understand a mechanism of the earthquake and the present condition of the fault. Surface ruptures intermittently observed along the northern part of Kamishiro fault in the southwest of the hypocenter (Katsube et al., 2015). Waveform inversion results, on the other hand, showed that large slip mainly distributed in the northeast of the hypocenter (Asano et al., 2015; Kobayashi et al., 2015; Shiba, 2015; Horikawa, 2015). Kase (2015) constructed dynamic rupture models composed of a single fault or two parallel faults, but could not simulate both the surface rupture distribution and the slip distribution on the fault. In this study, we investigate a fault model with a vertical fault as an initial crack between the two parallel faults, considering the difference between the focal mechanism (JMA, 2014) and the CMT solution (NIED, 2014).
Fault model of the main rupture and tectonic stress field are the same as Kase (2015). Based on the aftershock locations determined by Imanishi and Uchide (2015) and the analysis of the InSAR data (Yarai, 2015), fault strike is N20E, and dip angles of the deeper and shallower regions than 2 km are 60 and 45 degrees. The fault model is composed of two segments: the 10.1 km long northeastern segment corresponding to the large slip region, and the 13 km long southwestern one corresponding to the surface rupture. The fault model has a 2 km left-step with 2 km overlap. In this study, we add a vertical segment with an initial crack between the two main segments. The southern part of the fault reaches the earth's surface, while upper depth of the northern part is 2 km.
Principal stresses are proportional to depth. Azimuth of the maximum principal stress is N60W, and stress ratio is 0.42 (MEXT et al., 2004). The minimum principal stress is vertical, and equal to overburden load. We assume hydrostatic condition. The medium has two-layered structure with 2 km deep boundary, based on the subsurface structure model around the fault (NEID, 2003).
We calculate dynamic rupture processes by the finite-difference method (Kase, 2010), assuming the slip-weakening friction law. The preliminary results show that a rupture initiated on the vertical segment promotes rupture propagation toward the deep portion on the northeastern segment and the shallow portion on the southwestern segment, which agrees with the rupture process of the 2014 northern Nagano earthquake.

Keywords: dynamic rupture, 2014 northern Nagano earthquake, numerical simulation

 

# Relationship between various Source Characteristics and Slip Distribution determined by Source Process Analysis with Teleseismic Body-Wave

*Kenichi Fujita[1], Akio Katsumata[1], Koji Sakoda[2]

1.Meteorological Research Institute, 2.Japan Meteorological Agency

1. Introduction
We have examined optimized preset parameters for automate source process analysis with teleseismic body-wave, and we have become possible to preset optimized parameters based on scaling law without trial and error by analysts.
Then, we compared semi-automatic analysis (automatic analysis except for selecting stations and picking up initial P-wave) with manual analysis, and we confirmed that results were roughly consistent with each other for many events regardless of event magnitude. But, there were differences of slip distribution between semi-automatic analysis and manual analysis for some events.
We examine source characteristics which would reflect differences of slip distribution by comparing with aftershock distribution, tsunami source area, etc.

2. Analysis Methods
We used the same program package as Iwakiri et al. (2014) for analyzing source process with teleseismic body-wave. We used broadband waveform data which were downloaded from IRIS DMC HP, and set sampling time and band-pass filter depending on event magnitude. We used epicenter data of JMA for events in and around Japan, and USGS for events in other areas. We used focal mechanism data of JMA for events in and around Japan, and GCMT or others for events in other areas. Hypocenter was set at center of assumed fault plane, and subfaults size and number were set depending on event magnitude. Source-time function were set with triangle functions, and number of basis function and rise time were set depending on event magnitude. Analysis time was set at sum of time necessary for rupture front arriving at most distant subfault (from hypocenter) and time destruction allowed at subfault. Velocity structure for Green's functions were set based on the IASP91 model, and the CRUST2.0 model for near hypocenter. We used the ABIC (Akaike (1980)) for temporal and spatial smoothing constraints, and set hyperparameters as ABIC value become minimum. Maximum rupture speed was set at 0.72 times of S-wave velocity from empirical relationship of Geller (1976).

3. Comparing Methods
(1) We investigated number of aftershock on subfaults, and compared with slippage.
(2) We calculated crustal deformation of land or seafloor surface from slip distribution, and compared with tsunami source area.
(3) We investigated location of the maximum aftershock and slip distribution of the maximum aftershock, and compared with slippage.

Keywords: Source Process Analysis, Slip Distribution

 

# Simulation of Recurring Earthquakes along the Japan Trench

*Kenichi Fujita[1], Fuyuki Hirose[1], Kenji Maeda[1]

1.Meteorological Research Institute

## 1. Introduction

Magnitude (M) 7-8 earthquakes have been known to occur repeatedly along the Japan Trench by historical evidences. Recently the occurrence of the 2011 off the Pacific coast of Tohoku earthquake has proved the possibility of recurrence of M9 class earthquakes.

Basing on these data of the past earthquakes, we try to make the numerical simulation model reproducing magnitude (about 7-9) and recurrence interval (T) estimated for earthquakes recurring along the Japan Trench.

## 2. Methods

The target earthquakes that are known to occur repeatedly and we aim to simulated are the northern Sanriku earthquake (M~8.0, T~100 years), the Miyagi-oki earthquake (M~7.5, T~40 years), the near trench southern Sanriku earthquake (M~8.0, T~110 years), the Ibaraki-oki earthquake (M~7.0, T~20 years), and the type of The 2011 off the Pacific coast of Tohoku earthquake (M~9.0, T~600 years). In addition, we tried to reproduce the characteristics of earthquakes near trench northern Sanriku (1896 Meiji-Sanriku earthquake of Mt~8.6-9.0) and around Fukushima-oki (1938 Fukushima-oki earthquake swarm of M~7.4) whose repeatability, however, is not clear.

We used the equation of motion considering shear-stress reduction (Rice (1993)), and adopted the composite law (Kato and Tullis (2001)) for the rate- and state-dependent friction law. Analysis region was set largely enough to surround all asperities of the target earthquakes. We used the three-dimensional plate configuration of Nakajima and Hasegawa (2006), and set 17,507 triangular cells of the seize about 5 km. Subducting rate of the Pacific plate against land plate was put 8.0-8.2 cm/year from south to north referring to Wei and Seno (1998) etc. Frictional parameters (a, b, L) were chosen to reproduce magnitude and recurrence interval of the earthquakes by trial and error. We basically consider two types of parameter sets: Case 1 (background stable slip model), region surrounding asperities (background) is velocity strengthening ($a-b > 0$), Case 2 (hierarchical model), background is velocity weakening ($a-b < 0$).

## 3. Results

Magnitude and recurrence interval of earthquakes we simulated in our model as follows. In the case 1, the northern Sanriku earthquakes are (M~8.0, T~61-103 years), the Miyagi-oki earthquakes (M~7.4, T~30-74 years), the near trench southern Sanriku earthquakes (M~7.9, T~104-130 years), the Ibaraki-oki earthquakes (M~6.8, T~14-52 years), and the type of The 2011 off the Pacific coast of Tohoku Earthquake (M~8.3, T~203-232 years (the latter half magnitude of M8 class earthquakes occurred once every few times). It is noteworthy that near trench northern Sanriku earthquakes occurred a few years after the northern Sanriku earthquakes, and swarm-like Fukushima-oki earthquakes occurred in some cases.

In the case 2, the northern Sanriku earthquakes (M~7.9, T~66-140 years), the Miyagi-oki earthquakes (M~7.3, T~31-149 years), the near trench southern Sanriku earthquakes (M~7.8, T~120-216 years), and Ibaraki-oki earthquakes (M~6.8, T~9-51 years), and the type of the 2011 off the Pacific coast of Tohoku earthquake (M~8.5, T~294-526 years (M9 earthquakes occurred once every few times). In this case, near trench northern Sanriku earthquakes didn't occur, but swarm-like Fukushima-oki earthquakes occurred in some cases.

 

In the future studies, we will examine frictional parameters further in order to make more realistic numerical simulation models.

Keywords: Simulation of Recurring Earthquakes, The 2011 off the Pacific coast of Tohoku Earthquake

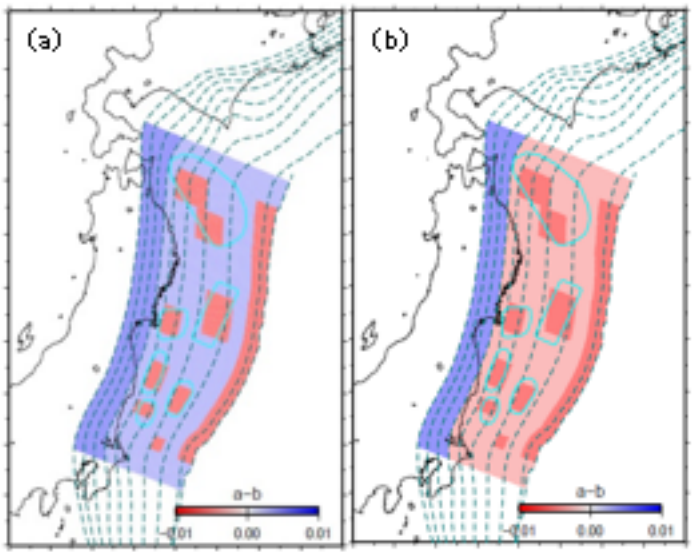


Figure 1. Friction parameter (a - b) (a) background stable slip model (b) hierarchical model

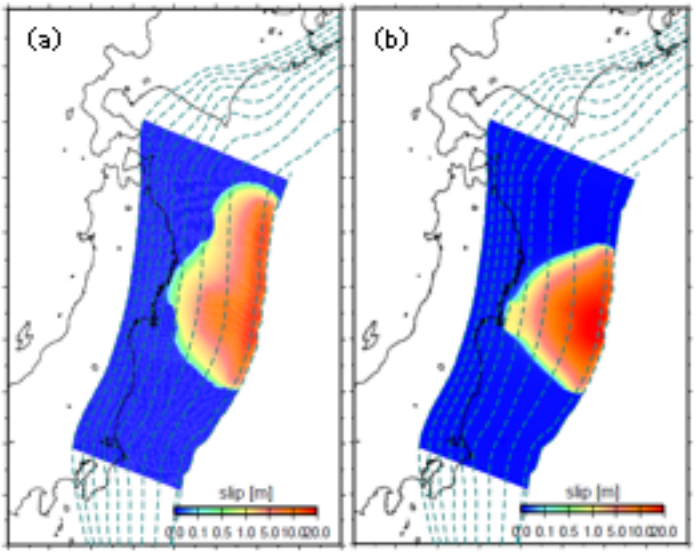


Figure 2. Slip distribution (a) background stable slip model (b) hierarchical model

 

# Simulation of the Nankai earthquake cycle -Quasi-dynamic discrete-cell model incorporating rate-weakening due to thermal pressurization-

*Yugo Ozaki[1], Kazuro Hirahara[1]

1.Graduate School of Science, Kyoto University

Along the Nankai Tough, great earthquakes have historically recurred, causing devastating disasters in southwest Japan, and the next Nankai earthquake is anticipated to occur in the first half of this century. The recurrence times of the Nankai earthquakes vary from 90 to 250 years. The source region extending from off-Shikoku to off-Tokai regions is divided into five segments. The segments complicatedly slip at each event; all five segments seismically slip, and some segments seismically slip with delays or sometimes not slip (Ishibashi, 2004). Moreover Seno [2012] re-examined the historical sequences and proposed that the source region is characterized into a seismic-b, tsunami-b and geodetic-b areas where seismic waves, tsunamis and crustal deformations are dominantly generated, respectively, and the historical events are grouped into the Ansei-type or the Hoei-type. His model might explain the complexity of historical sequences, but we need some verification. We execute earthquake cycle simulations to reveal the complexity.
In this study, we take a boundary element method to simulate earthquake cycles following the rate- and state-dependent friction law. Setting spatially heterogeneous friction parameters on the fault may not reproduce the complex historical sequences, and another factor should be introduced in the numerical model. Noda and Lapusta [2010] focused on the thermal pressurization (TP) that the increases pore fluid pressure at the shear zone due to frictional heating and showed that the interaction of two patches with spatially heterogeneous hydraulic parameters produces complex earthquakes cycles. The goal of this study is to reproduce the complex sequences by introducing TP in addition to spatially heterogeneous frictional parameters in the model. Their simulation include the dynamic rupture process, but in this study we use the radiation damping (Rice,1993) to simulate quasi-dynamically for reducing the computational cost. The quasi-dynamic approximation may cause the underestimation of TP effect, which should be examined in future.
TP increases the effective normal stress, and then the friction drops coseismically. Therefore the amount of coseismic slip increases and the recurrence interval gets longer than that without TP. For calculating the temporal change in pore fluid pressure by TP, we use the convolution form proposed by Bizzari and Cocco [2012] which enables us to take a longer time step than that in the case solving numerically the diffusion equation. However, the numerical cost of convolution calculation is also enormous. Accordingly, it is quite difficult to execute cycles of great earthquakes such as Nankai earthquakes as in a continuum medium, considering also the numerical cost of calculating interaction between a huge number of cells. Hence we consider a conceptual model similar to the block and spring model [Mitsui and Hirahara, 2004]. The numerical cost using their model is relatively smaller even when taking account of thermal pressurization. They set five blocks corresponding to five segments and assign properties to respective blocks; for example, dip angles, plate convergence rates and frictional parameters. In this study we calculate slip response functions by the code of Okada [1992] for elastic interactions between cells instead of springs, which is called a discrete cell model. Because we found only five cells produce almost no interactions, we divide each cell to a number of cells along its subduction direction. In addition to a variety of frictional parameter settings, we apply TP to specific cells and we compare the calculated patterns of earthquake cycle with the historical sequences of the Nankai earthquakes. This conceptual model and the resultant earthquake cyclers are expected to contribute to the actual reproduction of the Nankai earthquake sequences by simulating not as a discrete cell model but as a

 

continuum model.

Keywords: Nankai Trough, simulation of earthquake cycle, a boundary elementary method, pore fluid pressure, thermal pressurization

 

# Simulated precursory large aseismic slip at the deeper extension of the seismic region along the Nankai Trough, SW Japan

*Makiko Ohtani[1], Nobuki Kame[1], Masao Nakatani[1]

1.Earthquake Research Institute, The University of Tokyo

At the subduction zone along the Nankai Trough, SW Japan, large earthquakes around M8 had occurred repeatedly. Their intervals (around 100–200 years) have been identified precisely from old historical documents combined with geological surveys (*Sangawa*, 2011). The most recent events occurred in 1944 (the Showa To-Nankai EQ.) and 1946 (the Showa Nankai EQ.) when modern satellite geodetic networks had not been developed yet.
The existence of short-term aseismic processes before the 1944 and 1946 events has been inferred from the leveling or interview records. Two-times level difference measurements showed the displacement of north down before the 1944 event (*Mogi*, 1986), and the water level of some wells were reported to have dropped before the 1946 event (*Sato*, 1982). These phenomena were observed within several days before the earthquakes, and each could have been caused by 2 m slip on the plate interface at the deeper extension of the seismic region before each event (*Linde and Sacks*, 2002).
In this study, we simulate the cycle of large earthquakes in a quasi-dynamic 2D model to investigate aseismic slip acceleration in the deeper extension of seismic fault. We consider a flat plate interface with a shallow dipping angle of 15° for the depth 0–60 km mimicking the Nankai Trough. Following *Nakatani and Scholz* (2006) and *Yoshida et al.* (2013), we introduce an intrinsic cut-off time for healing into the state evolution law of the rate-and-state friction. The intrinsic time leads to a corresponding cut-off velocity ($V_{cx}$) beyond which velocity strengthening occurs. We assume that $V_{cx}$ is depth dependent (1–$10^{-9}$ m/s). We show that this depth variation in $V_{cx}$ can possibly produce large aseismic slip.
In our simulation, the bottom part of the fault below the deeper extension exhibits a constant slip rate loaded by a subducting plate velocity (4.5 cm/year). This bottom slip drives the adjacent deeper locked part and aseismic slip starts to accelerate. Because of the introduction of low $V_{cx}$ there, the slip cannot monotonously accelerate to seismic slip at the same depth. Instead, the aseismic slip propagates to the shallower part where the slip accelerates following the increasingly higher $V_{cx}$ at the depth, and finally reaches to seismic slip at the shallow part with the large $V_{cx}$. The seismic slip starting at shallow part then propagates bilaterally to the shallower and deeper parts, and develops into a large earthquake. For example, the point at 20 km depth starts to slip aseismically 5.4 days before the earthquake and 54% of the slip occurs as the precursory aseismic slip. The deeper part produces the longer-lasting aseismic slip with the smaller velocity.
This simulated aseismic slip may correspond to the several-days precursors of the 1944/1946 events. Our results also suggest that the observed short-term aseismic slip acceleration is a part of the longer-term aseismic slip that has started at deeper parts, which may be detected at the next To-nankai/Nankai earthquakes with the help of recently installed modern observation networks (Do-Net, Hi-Net, and GEONET) around the Nankai region.
This study was supported by the Ministry of Education, Culture, Sports, Science and Technology (MEXT) of Japan, under its Earthquake and Volcano Hazards Observation and Research Program.

Keywords: Nankai Trough, precursory slip, cycle simulation

 

 

# Numerical simulation of slow slip events, considering the effect of earth tide

*Takanori Matsuzawa[1], Yoshiyuki Tanaka[2], Bunichiro Shibazaki[3]

1.National Research Institute for Earth Science and Disaster Prevention, 2.Earthquake Research Institute, the University of Tokyo, 3.Building Reserach Institute

Several studies reported that occurrence of slow slip events (SSEs) in the Nankai region is affected by earth tide (e.g., Nakata et al., 2008; Tanaka and Ide, 2014). The effect on the SSEs is also examined by numerical studies (e.g., Hawthorne and Rubin, 2013). We have studied the behavior of SSEs during seismic cycles in numerical simulations (e.g., Matsuzawa et al., 2010), and suggested that recurrence intervals may decrease at the later stage in a seismic cycle. In this study, we examined the behavior of SSEs during seismic cycles, considering the effect of earth tide.
Our numerical model is similar to our previous study with a flat plate interface (i.e., Matsuzawa et al., 2010). A plate interface is expressed by 40,000 small rectangular elements. A rate- and state-dependent friction law with a cutoff velocity is adopted as the friction law on each element. In the region deeper than short-term SSEs, low cutoff velocity ($10^{-6.5}$ m/s) and low effective normal stress are assumed. In the following section, we show an example in the case of sinusoidal stress perturbation at the period of M2 tide (i.e. 12.42 hours) with 2 kPa peak-to-peak amplitude, which has the phase that maximum shear stress coincides with minimum normal stress.
In the numerical result, introduction of earth tide slightly decreases recurrence interval of megathrust earthquakes, for example, from 106.5 years to 106.2 years between first and second large earthquakes, and from 106.5 years to 105.9 years between second and third large earthquakes. This suggests that the earth tide can also affect the recurrence intervals of large earthquakes.
In terms of short-term SSEs, the recurrence intervals decrease during a seismic cycle both in the cases with and without tidal effect. The difference between these two cases is not clear. We note that SSEs are detected on each rectangular element, if displacement exceeds 5 mm during episodic slip with more than twice of subduction velocity. In terms of the relationships between the occurrence of SSEs and phase of tides, the distribution of occurrence times of SSEs shows a peak around the phase with maximum shear stress and minimum normal stress. The SSEs, which occur between -30 and 30 degrees from this phase, are 22.7%, 22.7%, and 22.2% of the total number of SSEs, during the period of 5-35 years, 35-65 years, and 65-95 years after large earthquakes, respectively. These values are higher than the identical ratio of 16.7% with no relevance. Our numerical simulation also suggests that the stress perturbation by earth tide can affect the occurrence of SSEs, although the change during seismic cycle is not clear in this case.

Keywords: Slow slip event, Numerical simulation, Earth tide

 

# Dependencies of pore pressure and fracture distribution on elastic wave velocities for thermally cracked rocks : Implications for high Vp/Vs zone related to slow slip events along plate boundary

Kaya Nishimura[1], *Shinichi Uehara[2], Kazuo Mizoguchi[3], Kohei Seto[2], Kenji Kawashima[2]

1.Graduate School of Science, Toho University, 2.Faculty of Science, Toho University, 3.Central Research Institute of Electric Power Industry

Seismic studies have found that there are high Vp/Vs ratio regions in oceanic crusts at subducting oceanic plates (e.g., Cascadia (2.0-2.8) (Audet et al., 2009), Nankai trough (> 2.03) (Kodaira et al., 2004)), and the correlations between the location of high Vp/Vs and slow slip zone have been pointed out by several studies. Christensen (1984) indicated that high pore pressure may cause high Vp/Vs. It is also known that Vp/Vs also depends on porosity or pore structures (fracture distributions). However, the relationships between Vp/Vs, pore pressure, porosity and fracture distribution have no investigated in detail for rocks composing oceanic crusts.
This study reports the results of measurements of Vp and Vs (transmission method) at controlled confining and pore pressure and estimation of Vp/Vs ratio for thermally cracked dolerite and relation between Vp/Vs, pore pressure and fracture distributions. Confining pressure was constant (50 MPa) and pore pressure was decreased from 49 to 0.1 MPa and then increased to 49 MPa. We did measurement with an intact rock specimen (0.5% in porosity) and the rock specimens heated under 300, 500 and 700°C for 24 hours (2.1%, 3.4% and 3.5% in porosity, respectively). Rock specimens heated under 500 and 700°C were reddish in color, which suggested a possibility that not only cracking but also oxidizations of rock forming minerals might affect elastic velocities. Therefore, we operated elastic velocity measurements under atmospheric pressure with rock specimens heated under 500 and 700°C at air (an oxygen concentration is around 21%) and at nitrogen conditions (an oxygen concentration is less than 0.5%), and revealed that the effect of oxidization on Vp/Vs is several times less than the effect of heating-temperature conditions.
In this experiments, for the intact rock specimen and specimen heated under 300°C, Vp and Vs was almost constant at any pore pressure, and for specimen heated under 300°C, Vp/Vs was 1.7 to 1.8, which is less than the high Vp/Vs ratio observed at oceanic crusts of subducting plates. On the other hand, for specimens thermally cracked under 500 and 700°C, Vp/Vs increased as pore pressure was increased (effective pressure was decreased), and was more than 2 when pore pressure was over 40 MPa and 30 MPa, respectively. This results indicate that Vp/Vs is not over 2 unless porosity is larger enough (approximately 3% for the results in this study), even if pore pressure is higher.
We also observed fractures in the specimens by using a microscope, and measured fracture densities. The fracture densities for the specimens heated under 500 and 700°C were larger than that of the intact rock specimen. There was no clear difference on the fracture density between the specimens heated under 500 and 700°C, but microscope observations revealed that there was differences on fracture distributions such that fine net-like fracture distributions or networks of intra-mineral fractures were observed more for the specimen heated under 700°C than that under 500°C. These features on fracture distributions might affect elastic velocities. In general, high Vp/Vs near slow slip zones tends to be simply interpreted as high pore pressure, but it may also be influenced by porosity and features of fracture distributions.
This work was supported by JSPS Grant-in-Aid for Scientific Research (Grant Number 26400492) .

Keywords: high Vp/Vs, laboratory experiment, fracture density, high pore pressure

 

 

# Effect of fault surface evolution on slow slip behaviors in large-scale biaxial experiments

*Futoshi Yamashita[1], Eiichi Fukuyama[1], Shiqing Xu[1], Kazuo Mizoguchi[2], Shigeru Takizawa[1], Hironori Kawakata[3]

1.National Research Institute for Earth Science and Disaster Prevention, 2.Central Research Institute of Electric Power Industry, 3.Ritsumeikan University

To investigate the preparation process preceding the main fast rupture under more realistic condition, we conducted stick-slip experiments using large-scale biaxial friction apparatus at NIED in Tsukuba, Japan. We used two rectangular metagabbro blocks as specimen, whose contacting area was 1.5 m long and 0.1 m wide. The experiments were repeatedly conducted with same pair of specimens, which means the fault surface evolved with the frictional slip. We successively conducted a set of three experiments under the condition of constant normal stress of 6.7 MPa and loading rate of 0.01 mm/s. All wear materials were collected after each experiment. To artificially accelerate fault evolution from one stage to the next, we applied fast loading with long slip displacement between a set of three experiments. As a result, we obtained three sets of the experimental result in different evolutional stages I, II and III; one and two fast-loading processes mentioned above were performed before the experimental sets in Stage II and III, respectively. In all experiments, we observed many stick-slip events, the number of which tended to increase with the maturity of the fault. Local strain array also showed slow propagation of shear stress drop, which was derived from slow slip before the main rupture. We found that the occurrence location of slow slip and its occurrence time relative to the main rupture, depend on the stage of fault evolution. In Stage I, both the temporal and spatial distributions of the slow slip occurrence were mono-modal, whereas a variety of occurrence times were observed in Stage II and III. The occurrence locations in Stage I and II look consistent with the initial normal pressure distribution on the fault, which was estimated from pressure sheet measurements (Fujifilm PRESCALE LW) just before each experiment; slow slips started to propagate from the location where the initial normal pressure is at a local minimum. On the contrary, we cannot find such clear relationship in Stage III, though some of the occurrence locations look related to the distribution of wear material generated with the frictional slip. These results suggest that the fault surface evolution may increase the complexity of slow slip behaviors.

Keywords: Slow slip, Fault evolution, Friction experiment

 

# Transient Frictional Behavior Observed in the Velocity-Stepping Test of Gabbro Conducted at Intermediate to High Slip Velocities

*Ryuji Nakano[1], Akito Tsutsumi[1]

1.Graduate School of Science, Kyoto University

Since Brace and Byerlee [1966] suggested that frictional stick-slip sliding plays an important role in seismic faulting, a number of friction experiments have been carried out. One of the greatest achievements is a proposal of rate- and state-dependent friction constitutive law by Dieterich [1978]. This law has been widely used for simulating earthquake cycles, but the law was originally proposed at low slip velocities of the order of sub-$mms^{-1}$, and it has not been clarified whether rate- and state-dependent friction constitutive law can be applied to frictional phenomena at seismic faulting slip velocities (the order of $ms^{-1}$).
In this study, we modified a rotary-shear friction apparatus at Kyoto University and performed a series of intermediate to high slip velocity friction experiment with velocity stepping by using this apparatus. In this experiment, we used a pair of hollow cylindrical gabbro blocks with an inner-diameter of 26 mm and an outer-diameter of 40 mm, and changed the rotation rate of the servomotor in this apparatus from one value to another; hereinafter we call the former value *IRPM* and the difference value between the former and the latter *ΔRPM*, respectively. We selected all the combinations of IRPM and ΔRPM throughout this experiment: a value of IRPM of either 10, 20, 50 or 100 RPM, and a value of ΔRPM of either 30, 80, 150, 200, 300 or 400 RPM. This experiment was carried out under a constant normal stress of 1.5 MPa.
The friction response to the imposed slip velocity steps is characterized by two strength peaks and slip-weakening phases that follow each of the peaks. Typical behavior of the transient was observed in the tests conducted at an IRPM value of 20 RPM and a ΔRPM value of 200 RPM. Rotation rate overshoots the target value once and is converged to the value while oscillating because of high value of the speed loop gain integration time constant of the servomotor in this apparatus during this experiment. Considering this servomotor behavior, the first strength peak is reached while the rotation rate is accelerating, and the second peak is reached when the rotation rate reaches its peak value. Interestingly to note, the transient behavior of friction response recorded in this study is similar to those observed in friction melting experiments [e.g., Hirose and Shimamoto, 2005]. There are many kinds of friction constitutive law, but existing friction constitutive laws may not describe this behavior. A constitutive model for frictional sliding that is capable of describing the transient behavior observed at intermediate to high slip velocity tests in this study is required to be developed.

Keywords: Friction experiment, Friction constitutive law, Intermediate to high slip velocity

 

# Frictional properties of pre- and post-subducting oceanic basement rocks

Ken Kohama[1], *Yujin Kitamura[2], Akito Tsutsumi[3]

1.Department of Earth and Environmental Sciences, Faculty of Science, Kagoshima University, 2.Department of Earth and Environmental Sciences, Graduate School of Science and Engineering, Kagoshima University, 3.Graduate School of Science, Kyoto University

On the faults in the subduction plate boundary, fault slips when the shear stress exceeds the strength of the rock interface between the hanging and footwall. Seismic slip is associated when the frictional strength decreases with the slip. The up-dip limit of the seismogenic zone coincides with the stepping down of the décollement to the oceanic basement. Seismogenic process is thought to undergo in the upper part of the oceanic crust (Kimura and Ludden, 1995; Bangs et al., 2009). Tectonic mélanges of the Shimanto belt which is formed along the plate boundary fault zone (Kitamura et al., 2005) contains basalts with cataclastic shear zones. To understand the seismogenic process, therefore, basalts are key material and it is essential to know their frictional properties. Here we performed frictional experiment on the basalts from pre-subduction drilled core in the Nankai trough and post-subduction outcrop in the Shimanto belt.
We performed friction experiments using the rotary shear, an intermediate to high velocity frictional testing apparatus in Kyoto University. Basalt samples were taken from IODP Expedition 333 Site C0012 as pre-subduction materials (C12G8R, C12G10R) and from the Mugi tectonic mèlange as postsubduction material (MBN-3). We performed constant low velocity test with normal stress of 2 MPa and rotational speed of 0.012 r.p.m with all three samples, and velocity stepping test to evaluate the velocity dependence with two samples (C12G8R, MBN-3) with normal stresses of 2 MPa and 5 MPa.
Results of the constant low velocity test showed the steady frictional coefficient of C12G8R, C12G10R and MBN-3 ranging from 0.70 to 0.84 (average 0.76), from 0.60 to 0.79 (ave. 0.67) and from 0.50 to 0.63 (ave. 0.57), respectively. On the velocity stepping tests, C12G8R and MBN-3 with normal stress of 2 MPa showed neutral depencence of the friction coefficient to the velocity. But, C12G8R with normal stress of 5 MPa showed velocity strengthening behavior and MBN-3 with normal stress of 5 MPa showed velocity weakening behavior.
The constant low velocity tests revealed that the frictional coefficient of MBN-3 is lower than those of C12G8R/C12G10R. This implies that the post-subduction basalt is essentially weaker. From the results of velocity stepping tests, pre-subducting basalt (C12G8R) without preexisting gouge on the interface (5 MPa, menu 1) showed notable velocity strengthening. Other runs at 5 MPa are velocity neutral or strengthening. On the other hand, post subducting basalt (MBN-3) showed velocity weakening at 5 MPa, menu 1 and 2. These results suggest that the subducting oceanic crust progressively changes its frictional property that enables the rocks to be potent in seismogenesis may leading to the stepping down of the decollement to the oceanic basement at the up-dip limit of seismogenic zone.

Reference

BANGS, N. L. B., et al. Broad, weak regions of the Nankai Megathrust and implications for shallow coseismic slip. *Earth and Planetary Science Letters*, 2009, 284.1: 44-49.
KIMURA, Gaku; LUDDEN, John. Peeling oceanic crust in subduction zones. *Geology*, 1995, 23.3: 217-220.
KITAMURA, Yujin, et al. Mélange and its seismogenic roof décollement: a plate boundary fault rock in the subduction zone—an example from the Shimanto Belt, Japan. *Tectonics*, 2005, 24.5.

 

Keywords: Nankai Trough, Shimanto Belt, Frictional experiment, basalt, velocity weakening

 

# Evolution of fault surface state during frictional weakening of quartz rocks

*Hirotaka Iida[1], Akito Tsutsumi[1]

1. Graduate School of Science, Kyoto University

Siliceous rocks such as novaculite and quartzite display dramatic weakening of frictional strength at slip velocities of >1 mm/s [Goldsby and Tullis, 2002; and Di Toro et al., 2004].It has been suggested that the frictional weakening likely resulted from production and shearing of hydrated amorphous silica layer along a fault in quartz rocks. However, there exists little information on the frictionally-generated material; consequently the mechanism of the weakening remains poorly understood. In this study, to better characterize the state evolution of the fault surfaces of quartz rocks during the slip-weakening, we have performed SEM and stereo microscope observation of the fault surface and XRD analysis of the gouge formed on the fault.
All the experiments in this study were conducted using a rotary-shear, intermediate-to high-velocity friction testing machine in Kyoto University. The test samples used for the friction experiments were chert from the Tamba Belt, northern Kyoto prefecture, Japan, which is a Jurassic accretionary complex, and single crystal of quartz (a synthetic crystal). A pair of solid cylinders with a ring-shaped end surface (inner and outer diameter of 5 mm and 25 mm) was cored from the samples. Experiments were carried out under a constant normal stress condition of 1.5 MPa and at slip velocities of 105 mm/s, 10.5 mm/s and 1.05 mm/s.
Experimental results reveal that slip-weakening occurs at all the tested slip velocity conditions. At slip velocity of 105mm/s, both of the quartz and the chert specimens show very low friction coefficient value of 0.1 to 0.2 after the slip-weakening. The values of the slip-weakening distance ($D_c$) of this study are 0.2 to 0.3 m for the quartz specimens and 0.7 to 1.5 m for the chert specimens, respectively. These values are by an order of magnitude smaller than the $D_c$ value reported in Hayashi and Tsutsumi [2010]. The $D_c$ value appears to depend on the parallelism of the initial fault surfaces.
Fault surfaces after the experiments are covered by white, fine-grained gouge. The SEM observation reveals the development of asymmetric flake-like structure on the sliding surface, which is characterized by tearing of the surface material with approximate size of 100 to 300 μm. The XRD analyses reveal that only the chert specimen that had slipped for large displacement after the slip-weakening behavior contains amorphous material. This result suggests that the gouge material formed during the slip-weakening period is not amorphous.

 

# Foreshock activity during stick-slip experiments of large rock samples

*Yushi Tsujimura[1], Hironori Kawakata[1], Eiichi Fukuyama[2], Futoshi Yamashita[2], Shiqing Xu[2], Kazuo Mizoguchi[2,3], Shigeru Takizawa[2], Shiro Hirano[1]

1.Ritsumeikan University, 2.NIED, 3.CRIEPI

For inland earthquakes such as the 2007 Noto Hanto earthquake (Doi and Kawakata, 2013) and the 2008 Iwate-Miyagi earthquake (Doi and Kawakata, 2012), foreshocks were reported to occur in the vicinity of main shock hypocenter. Moreover, for interplate earthquakes such as the 2011 off the Pacific coast of Tohoku earthquake (Kato, et al., 2012) and 2014 Iquique earthquake in Chile (Yagi et al., 2014), migration of foreshocks toward the main shock hypocenter was detected in one month before the main shock. In order to understand the generation mechanism of foreshocks, it is important to investigate under what environments foreshocks occur.
Since 2012, stick-slip experiments have been carried out using a large-scale biaxial friction apparatus at NIED (e.g., Fukuyama et al., 2014). Based on the experimental result that foreshocks were detected only in the later period of each run, Kawakata et al. (2014) suggested that the foreshocks occur only after the generation of gouge. In this study, we carried out a series of stick-slip experiments with and without pre-existing gouge along a fault plane to confirm if fault gouge affects the foreshock activity. When foreshocks are detected, we estimate the hypocenter locations of foreshocks.
We used two rectangular metagabbro blocks to make the simulated fault plane, whose dimension was 1500 mm long and 500 mm wide. The experiments were conducted under normal stress of 1.33 MPa and loading speed of 0.01 mm/s up to approximate slip amount of 8 mm. During each experiment, we continuously measured elastic waves to detect foreshocks. The sensor distribution is shown in the figure below. Gouge materials were prepared naturally during preceding experiments whose sliding speed was as high as 1 mm/s.
To roughly detect foreshock activity, we calculated cumulative amplitude of continuous waveform data every 0.01 seconds. During an experiment without pre-existing gouge materials (LB13-004), a few foreshocks were detected. On the other hand, during an experiment with pre-existing gouge materials (LB13-007), much more foreshocks were detected. Then we estimated hypocenters of foreshocks for a stick-slip event (event 44) in LB13-007. Although the initial phases of the main shock were contaminated due to the coda wave signals of preceding foreshocks, the hypocenter of the main shock was roughly estimated near the right end of the fault plane. Foreshocks began to occur in the left half of the fault plane, but most of later foreshocks occurred near the right end. Therefore, we confirmed that foreshock activity was high when gouge materials were present along a fault plane, and found a similar hypocenter migration of foreshocks toward the main shock hypocenter, which was reported for interplate earthquakes.
In the future, we shall examine the data obtained from other experiments to confirm if the aforementioned features are common.
Acknowledgments: This work was supported by NIED research project “Development of monitoring and forecasting technology for crustal activity” and JSPS KAKENHI Grant Number 23340131.

Keywords: large-scale biaxial experiments, foreshock activity, fault gouge

 

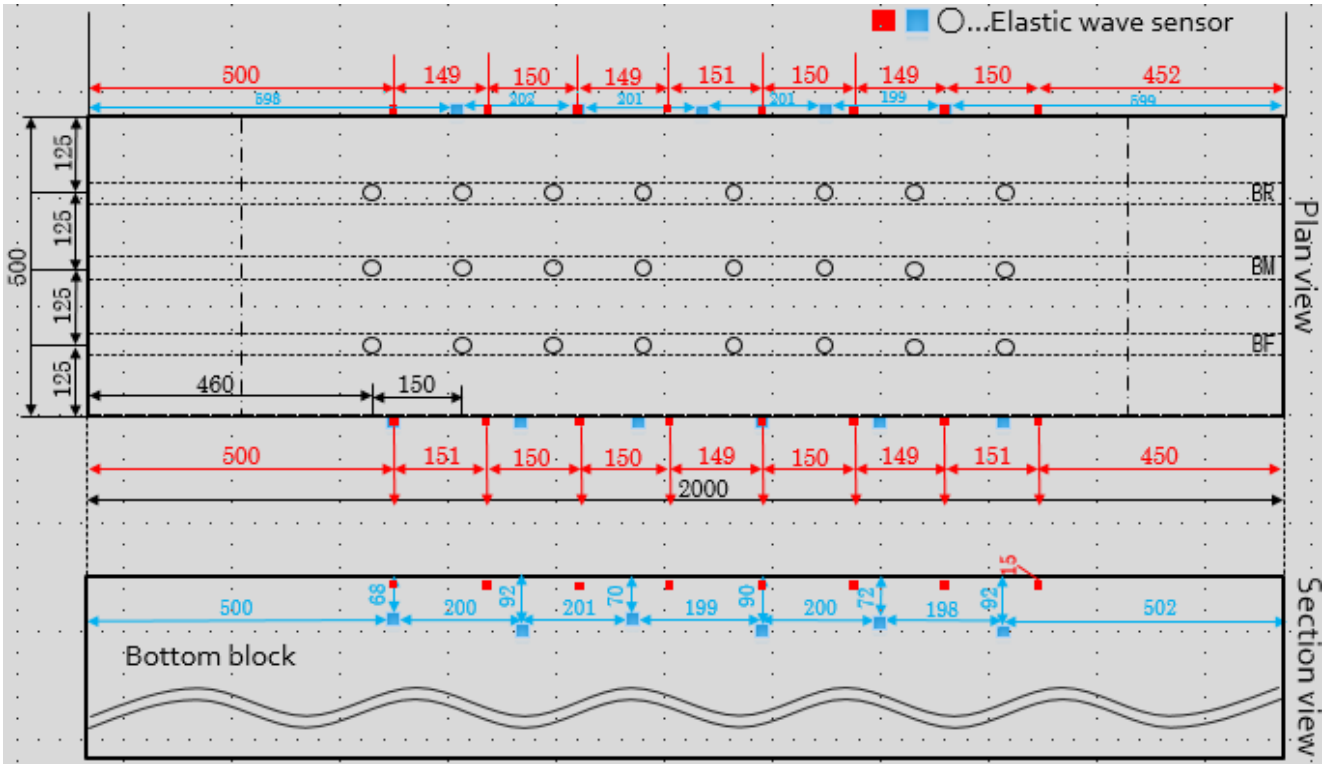


 

# Frictional behavior of smectite-bearing fault gouges in large displacement frictional experiments under constant pore pressure

Tomoaki Kawai[1], *Akito Tsutsumi[1]

1.Graduate School of Science, Kyoto University

Frictional properties of smectite-bearing material at large displacements should provide valuable information for the stability of slip in the shallow parts of subduction zone faults. However, most of the previous experiments are limited by the amount of displacement that can be achieved and the frictional behavior at large displacements remains poorly understood. In this study, we have conducted large displacement friction experiments on mixtures of montmorillonite and quartz at constant pore pressure. Our purpose of this study is to investigate the correlations between gouge textures and frictional velocity dependence of smectite-bearing faults.
We examined frictional behavior and internal textures of simulated gouge samples composed of montmorillonite/quartz mixtures. Two different compositions of the gouges were tested: mixtures of montmorillonite/quartz = 20/80 (abbreviated as Mnt20/Qtz80) and 40/60 wt% (Mnt40/Qtz60), respectively. We sheared the gouges in rotary shear to displacements of more than 1 m at a normal stress of 10 MPa and at a constant pore pressure of 5 MPa. During the shearing, these gouges were subjected to velocity step changes to examine the velocity dependence of friction for a range of slip velocities $v$ from 0.003 to 0.3 mm/s.
Results of the experiments reveal influences of the composition, displacements and slip velocities on the frictional behavior. Both Mnt20/Qtz80 and Mnt40/Qtz60 gouges show slip-hardening behavior. Positive friction velocity dependence was observed in both gouges at short displacement for all the tested slip velocities. At large displacement ($v$ > 30 mm), Mnt20/Qtz80 gouge shows negative friction velocity dependence for all the tested slip velocities. On the contrary, friction of Mnt40/Qtz60 gouge exhibits negative velocity dependence for lower velocities (0.003 mm/s to 0.03 mm/s) and positive velocity dependence for higher velocity stepping (0.03 mm/s to 0.3 mm/s). The SEM observation of the Mnt20/Qtz80 gouge reveals that montmorillonite particles are agglomerated initially to form montmorillonite-filled matrix domains. With continued displacement, the agglomerated distribution of montmorillonite becomes to be disaggregated; eventually the montmorillonite particles are incorporated into the fine-grained matrix of the gouge. Grain size of quartz decreases with displacement, during which change the grain shape of the quartz becomes to be more rounded. It appears that increasing degree of size reduction of quartz grains and a more scatter distribution of montmorillonite particles correlate with a more negative velocity dependence of friction.

Keywords: velocity dependence of friction, montmorillonite, large displacements

 

# Experimental demonstration for blackening of pseudotachylyte

*Yuki Nakano[1], Shunya Kaneki[1], Tetsuro Hirono[1]

1.Department of Earth and Space Science, Graduate School of Science Osaka University

Pseudotachylyte, basically formed by frictional melting at earthquake, sometimes shows various colors of not only black but also of greenish black and grayish black. The color might be correlated to the mineral assemblage, slip parameter, and environmental condition, but such relationship has not yet been investigated. We here demonstrated to form pseudotachylyte by using high-temperature furnace on the artificial mixture samples of quartz, albite, biotite, and chlorite. The melted product after heating the mixture of quartz and albite at 1300 °C did not show the blackening, whereas the products using the mixtures with 10 wt.% biotite and/or 10 wt.% chlorite became remarkably black. By taking consideration into the SEM-ESD data, we concluded that Fe-bearing minerals plays an important role for the color transition, especially, blackening in pseudotachylyte.

Keywords: pseudotachylyte, blackening

 

# Formation of pseudotachylyte in the lower crust plastic regimes: Evidence from the Woodroffe thrust, central Australi

*Takako Satsukawa[1], Aiming Lin[1]

1.Department of Geophysics, Division of Earth and Planetary Sciences, Kyoto University

Most reported fault-related pseudotachylytes are cataclasite-related, which have formed at shallow depths in brittle dominated seismogenic fault zones by both frictional melting and crushing mechanisms. Pseudotachylyte has also been described in association with mylonitic rocks having formed in deep-level fault shear zones within the semi-brittle to crystal-plastic regimes. However, the mechanism of coseismic shear zone formation in the lower crust is still poorly understood.
A >3.0 km-wide pseudotachylyte generation zone including a 1.5 km-wide mylonitized shear zone marked by large volumes of sub-mm- to cm-scale pseudotachylyte veins is developed along the Woodroffe thrust (central Australia) (Lin et al., 2005; Lin, 2008). The pseudotachylytes display typical melt-origin features, including rounded and embayed clasts, spherulitic and dendritic microlites, and flow structures within a fine-grained matrix. Three types of pseudotachylyte are identified on the basis of deformation texture, vein morphology, and host rock lithology: cataclasite-related (C-Pt), mylonite-related (M-Pt), and ultramylonite-related (Um-Pt). The textural and structural relationships between these pseudotachylyte veins and wall rocks indicate multiple stages of pseudotachylyte veins that formed at different times and depths.
Preliminary works have been performed by Lin et al. (2005) and Lin (2008), which have reported large volumes of coexisting C-Pt, M-Pt, and Um-Pt in cataclastic and mylonitic rocks within individual shear zones along the Woodroffe thrust. The M-Pt and Um-Pt veins contain distinct evidence of ductile deformation, including flattened and aligned fragments of host rocks that were re-oriented parallel to the foliation within the mylonite and ultramylonite, as evidenced from the continuity of the foliation between the host rock and vein fragments. These M-Pt and Um-Pt veins generally cut across the mylonitic foliation, and can locally be traced back to parent veins oriented parallel to the mylonitic foliation. These overprinting structural relationships indicate tat repeated pseudotachylyte-generating events occurred within the crystal-plastic dominated shear zone and that the pseudotachylyte veins themselves were mylonitized during ongoing plastic deformation. Here, we describe the microstructural and chemical characteristics of pseudotachylytes and discuss the processes leading to coseismic shear zone formation in the lower crust.
References:
Lin, A. et al., 2005, Propagation of seismic slip from brittle to ductile crust: Evidence from pseudotachylyte of the Woodroffe thrust, central Australia. *Tectonophysics* 402, 21-35.
Lin, A., 2008. Seismic slip in the lower crust, inferred from granulite-related pseudotachylyte in the Woodroffe thrust, central Australia. *Pure and Applied Geophysics*, 165, 215-233.

Keywords: pseudotachylyte, mylonite, ultramylonite

 

# Structural and mineralogical characteristics of an ancient plate boundary fault in the Hidakagawa Formation, Kii Peninsula, Japan

*Takeaki Ogawa[1], Naoki Kato[1], Naoya Tonoike[1], Satoru Asayama[1], Shunya Kaneki[1], Yuki Nakano[1], Tetsuro Hirono[1]

1.Department of Earth and Space Science, Graduate School of Science, Osaka University

To understand the slip behavior of mega earthquakes along plate boundary faults, geological studies of ancient seismogenic subduction faults in onland accretionary complexes such as Shimanto have been performed in providing important information about the characteristics of the fault-zone materials. Because the trench-parallel heterogeneity in the slip behavior of subduction earthquake is important to estimate the magnitude of the rapture area in the Nankai Trough, a more investigation at various regions in the Shimanto is required.
We here targeted the mélange unit of the Hidakagawa Formation, distributed around the Mio region, Kii Peninsula, and performed structural analysis of the fault rocks on the field and laboratory-based analyses such as XRD and SEM. We found a localized slip zone accompanying the evidence of intense shearing and melting, which might corresponds to an ancient seismogenic fault in the subduction boundary.

Keywords: plate boundary fault, accretionary prism, Nankai trough

 

# Distribution and characters of fault system in micro earthquake swarm area in central part of the Shimane Prefecture, southwest Japan

*Hideki Mukoyoshi[1], Masayuki Takeshima

1.Department of Geoscience Interdisciplinary Graduate School of Science and Engineering, Shimane University

Along a zone of central part of the Shimane prefecture to northern central part of the Hiroshima prefecture, magunitude (*M*) 5 class earthquake have occurred 6 times. In this area, numerous micro earthquakes is observed until recent days. The micro earthquake swarm zone is linearly distributed and the direction is parallel to the aftershock area of the 2000 Western Tottori earthquake (*M* 7.3). The linearly distributed micro earthquake swarm zone may reflect existence of concealed fault. However, active fault has not been reported around the zones and relationship of distribution of the micro earthquakes and geological background is also unknown. The objective of this study is to reveal the geologic structure, distribution of fault system and the characters based on the field observation on an area of the micro earthquake swarm zone.
The late Paleogene granitic rocks of the Akana granodiorite and the Ijimi granite, the Hakami volcanic rock is exposed in the study area. Basalt-andesite dikes, rhyolite dikes, and aplite is intruded into the granitic rocks.
More than 100 faults were observed in this study area. The fault plane is generally WNW strike with steeply north-dipping and NE strike with steeply south-dipping. Most of NE trending faults developed along granitic rock and dykes or granodiorite and granite. Some mm to cm thick white, light green and brown fault gouge and several cm to m thick cataclasite were observed in the faults. Fault rock of boundary fault of the Akana granodiorite and the Ijimi granite was composed of the tens of cm thick light greenish fault gouge, several m thick cataclasite, fault breccia and dozens of m of altered damaged zone. Some acidic dykes were intruded into the altered damaged zone and these dykes were not deformed. In contrast, the WNW trending faults cut the dykes and some mm to several cm thick thin fault gouges were observed within the faults. Cataclasites were not observed from the WNW trending faults.
The NE trending faults observed in this study is relatively thick with fault gouge and cataclasite. These fault plane is nearly orthogonal to the distribution direction of the micro earthquake swarms and dykes in the altered damaged zone of those faults were not deformed. These result indicates that the NE trending faults were formed in geologic period and not active at the present stress field. In contrast, WNW trending faults were developed independently of boundary of lithofacies and most of them has thin fault gouge. The orientation and occurrence of WNW trending fault are similar to the faults reported from aftershock area of the 2000 Western Tottori earthquake (Kobayashi et al., 2003; Aizawa et al., 2005). These result suggest WNW trending faults are considered as the Riedel shear planes of main fault and formed in the present stress field.

 